

Asymmetric Double Quantum Dot Structure as Nanoscale Diode

Shakir A. A. AL-Saidi,

Alaa Ayad Khedhair Al-mebir

Department of Physics, College of Education of Pure Sciences, University of Thi-Qar, Nasiriyha ,Iraq

Emails: Shakir.hussain@sci.utq.edu.iq

alaaayad@eps.utq.edu.iq

Abstract:

In this studying, a nanoscale diode was proposing by using asymmetric double quantum dot structure attached to metallic electrodes. An asymmetric double quantum dot (ADQD) is used as a diode for rectification. Tight-binding model was adopting to describe our specimen, and our results depend upon steady-state forming to show charge transport. The theoretical computations for current and conductance as a function of the time, that encouraging common traits of the rectifications, were presented. The analysis may be helpful in fabricating nanoscale electronic devices.

Keyword: Nanoscale diode; double quantum dot; tight-binding framework; conductance current.

1. Introduction

Quantum influences surprising are appearing in semiconductors if electrons or holes are confined in small size by potential barriers. The de Broglie wavelength of the charge carriers is greater than the dimensions of the quantum confinement [1]. Quantum dots (or artificial atoms) have splitting energy levels and bandgap energy may be varying by changing the size [2]. The nano-scale semiconductor particles which composed of groups II to VI or III to V materials and have dimensions less than the exciton Bohr radius are called quantum dots [3]. The quantum dots exhibit electronic properties that depend on their size. Nanocrystals also exhibit quantum mechanical effects that provide new routes for the research. The asymmetric

double quantum dot (ADQD) structure is a good paradigm where the electron movement is trapped and the electronic transport gets coherent [2-4]. Asymmetric double quantum dot (ADQD) structure contains double QD which are asymmetry size and aligned serially.

In 1974, Aviram and Rather first theoretically suggested that electron transfer in a bridge system, and design a molecular rectifier consists of an organic molecule sandwiched between two metallic electrodes [5]. Following this work, several theoretical [6-14] and experiments [15-18] studies have been running about different bridges systems to show the actual automatism of electron transfer. In 1995, Imamura et al. proposed a new optical memory structure by using InAs quantum dots with various sizes, which led to multiplication memory density [19]. Unimolecular rectifiers are designed by using asymmetric anchoring groups [20].

There are tutorials have been investigating around the electronic features of QD [21]. charge transfer features are describable by several important parameters as the quantization of energy levels [22]. Double [23], triple [24] or more quantum dots are setting as complex systems [14] offers many quantum states that obvious themselves, e.g., in current rectification [25] and Pauli spin blockade [26]. The normal limit for reducing charge carrier intensity is individual charge nano electronics, where externals such as conductance and current may be adjusted with single charge accuracy [27-29]. The transmission probability of an electron passes through the ADQD structure can be controlled efficiently by changing the direction of the current or the polarity of voltage [25]. Except important appliances in nanotechnology, there are also ideal tools for checking scientific essential troubles in single and many- objects physics. The advantage of using ADQD as a diode is due to their nanoscale size, perfect operation. In addition to, this nanostructure consider as a ballistic conductor, because electrons propagate freely, that lead to reducing the resistance [30]. The rectification action occurs in asymmetric case but it disappears in the symmetric case, because in the first case the current passes in one way while in the second case the current passes in two ways only. The diode designed by ADQD will be one million times smaller in area than the corresponding digital logic circuits fabricated on conventional computer chips [31].

In this study, we propose a theoretical scheme to the possibilities of designing nanoscale diode. To assay the work of ADQD structure as a diode, we use this diode in the rectification process. All our numerical calculations have been done based on a tight-binding framework and the steady state formalism. The numerical results for the conductance and current depict the traditional characteristics of the rectification process. This work may be advantageous for fabricating nanoscale diode using ADQD structure.

2. MODEL AND THEORETICAL FORMULATION

2.1. Rectification process

By connecting ADQD structure with AC signal, see Fig. 1, it was found the ADQD structure act as a diode actively because it can rectify the AC signal very well. The AC input signal can be described as [32],

$$V(t) = V_0 \sin(\omega t), \quad (1)$$

where V_0 is the peak voltage, ω and t are the angular frequency and the time, respectively. The oscillation of AC input signal as a function of ωt is shown in Fig. 2.

From the spectra indicated in Fig. 4, it is evident that positive half- wave can pass through the circuit. This behavior occurs when the ADQDs structure in the diode is aligned as follows: the small quantum dot, which has a large energy gap, is first, the second is the big quantum dot which has a small energy gap. While negative half-wave of the AC input signal are suppressed by inverse locations of the ADQD structure, which act as an inverse biased diode that is required for rectification.

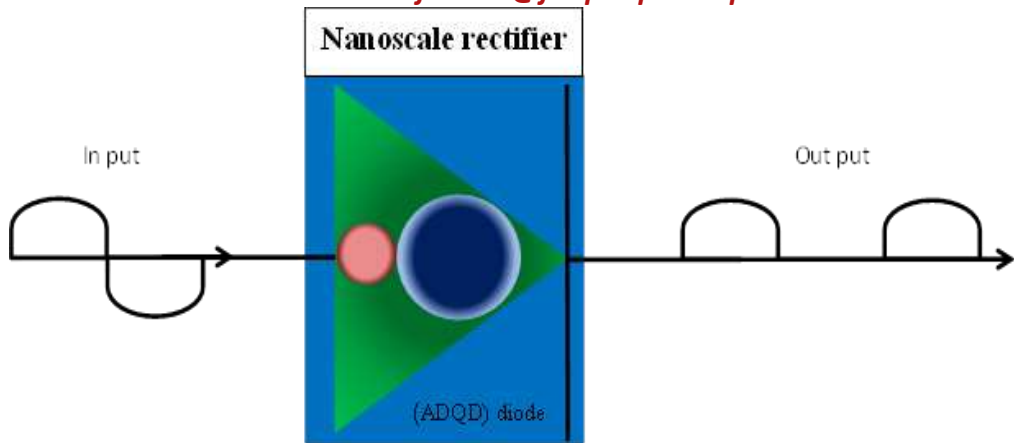


Fig. 1. The rectification process by using ADQD structure that acts as a diode. The diode attached to the source and drain.

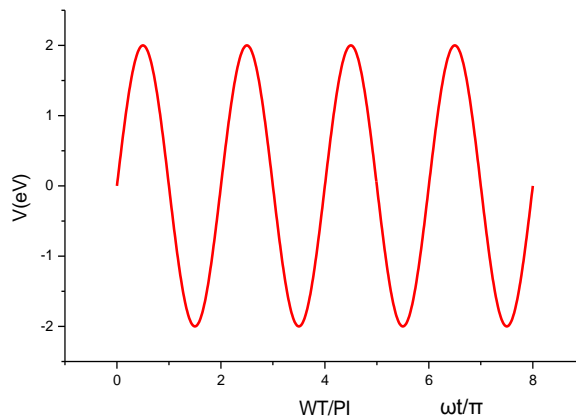


Fig. 2. Variations of AC input voltage signal as a function of the time.

In the rectifier which is connected to a single quantum wire, the current flows in one destination through every half wave of the AC input voltage.

2.2. Theoretical formulation

In the tight-binding treatment, the system may be parameterized into a series model, which takes into account an energy level of each QD and

coupling interaction between two QDs. The eigenvalues of the QDs are calculated by using tight binding model as following [33]:

$$E_j = E_Q - 2V_{mn} \cos\left(\frac{\pi j}{N+1}\right), \quad (2)$$

where E_Q is the energy level of the QD. V_{mn} is the coupling interaction among closest-neighboring QDs. N refer to the total number of the QDs.

The simplest tight binding treatment of the ADQD may be set up as a one-dimensional chain. Every connection between sites means the presence of a coupling interaction. The description of ADQD as a single site represents a simplification of wire model. We describe the system under consideration (that shown in Fig. 1) by deriving the following time-independent Hamiltonian (using Dirac's notations). We have derived the Hamiltonian equation that describes all the sub-systems interactions as following:

$$\begin{aligned} H = & E_D|D\rangle\langle D| + E_A|A\rangle\langle A| + \sum_{k_b} E_{k_b}|k_b\rangle\langle k_b| + \sum_{k_b} [(V_{Ak_b}|A\rangle\langle k_b| + h.c) \\ & + (V_{Dk_b}|D\rangle\langle k_b| \\ & + h.c) + h.c)] + \sum_{k_L} (V_{Dk_{L1}}|D\rangle\langle k_{L1}| + h.c) + \sum_{k_R} (V_{Ak_{L2}}|A\rangle\langle k_{L2}| \\ & + h.c), \quad (3) \end{aligned}$$

where the different indexes D , A , $L1$, $L2$ and b , that denote the donor, acceptor, first lead, second lead, and the QD with total number N , respectively. The index k_i is the energy wave vector with i which represents the indexes D , A , $L1$, $L2$ and b . E_i represents the energy level position and $|i\rangle$ and $\langle i|$ represent the ket and bra states, respectively. V_{ij} represents the coupling interaction between the subsystems i and j . We can derive the wave function system as following,

$$\psi(t) = C_D(t)|D\rangle + C_A(t)|A\rangle + \sum_{k_b} C_{k_b}(t)|k_b\rangle + \sum_{k_{L1}} C_{k_{L1}}(t)|k_{L1}\rangle + \sum_{k_{L2}} C_{k_{L2}}(t)|k_{L2}\rangle, \quad (4)$$

where $C_i(t)$ represents the linear expansion coefficients. The equations of motion for $C_i(t)$ can be obtained by using time dependent Schrodinger equation,

$$\frac{\partial\psi(t)}{\partial t} = -iH\psi(t), \quad (5)$$

Then by substituting equations (3) and (4) in (5) we obtain,

$$\frac{\bar{C}_A(E)}{\bar{C}_D(E)} = \frac{X_1(E)}{X_2(E)}, \quad (6)$$

where,

$$X_1(E) = V^{Ab} \Gamma_b(E) V^{bD}, \quad (7)$$

$$X_2(E) = E - E_A - \sum_{AL1} (E) - \sum_{Ab} (E), \quad (8)$$

here $\sum_{Ai}(E) = -i\Delta_{Ai}(E) + \Lambda_{Ai}(E)$, where $\Delta_{Ai}(E)$ is the broadening function, while $\Lambda_{Ai}(E)$ is the quantum shift function, where $i = L1, b$. Thus, the transmission amplitude and the transmission probability are respectively defined by [34]:

$$t(E) = \frac{\bar{C}_A(E)}{\bar{C}_D(E)}, \quad (9)$$

and ,

$$T(E) = |t(E)|^2, \quad (10)$$

The current through the active region may be computed by using the Landauer transport formula [35]:

$$I = \frac{2e}{h} \int_{-\infty}^{\infty} T(E) [f_{L1}(E) - f_{L2}(E)] dE, \quad (11)$$

the conductance, as long as the transmission probability is obtainable in our model calculation, by using the following formula [36]:

$$G = \frac{2e^2}{h} \int_{-\infty}^{\infty} dE T(E) \frac{\partial f_{\alpha}(E)}{\partial E}, \quad (12)$$

where $f_{\alpha}(E) = \{1 + \exp[E - \mu_{\alpha}/k_B T_{\alpha}]\}^{-1}$ is Fermi distribution function of electrons in the lead $\alpha = L1, L2$. The chemical potential of the lead α is μ_{α} with $\mu_{L1} = -V/2$ and $\mu_{L2} = +V/2$ where V is the bias voltage. The temperature T_{α} of the lead α . Here we use $T_{L1}=T_{L2}=T$ is fixed at 300 K, which means that the leads are in thermal equilibrium.

3. RESULTS AND DISCUSSION

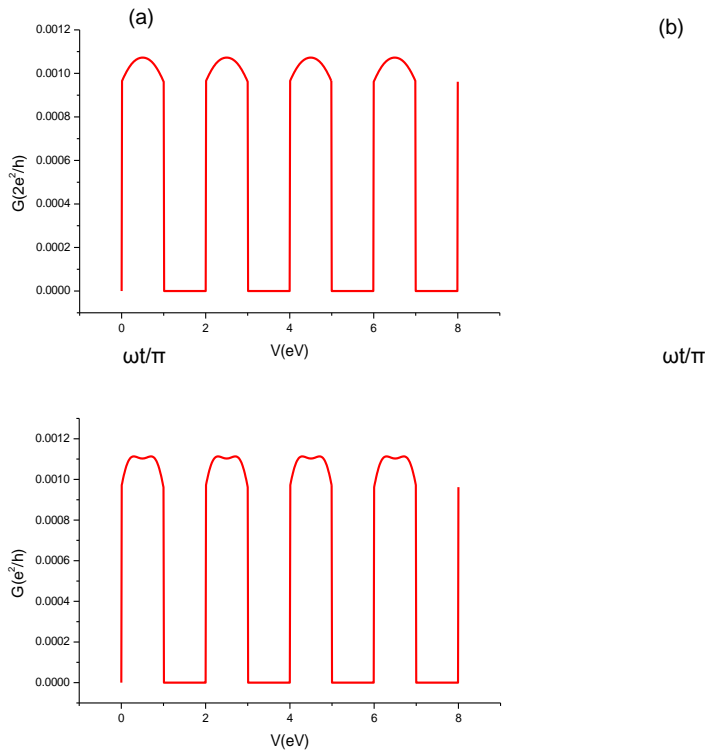
In beginning, we referred to the magnitude of factors which used for our numerical computations. The amplitudes V_0 of the AC input signals are set

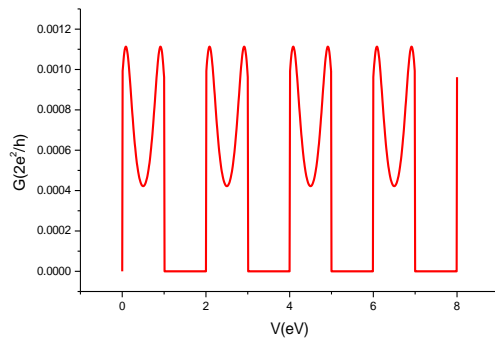
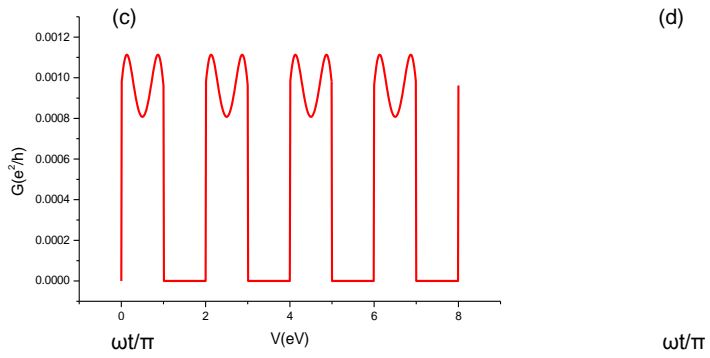
at different values fall among 0.1 eV to 2.0 eV. Closest-neighboring hopping strength V_{nm} is set to -0.1 eV. The coupling interaction of donor-bridge and acceptor-bridge are -0.01 eV. The balance Fermi energy E_F is at zero. The energy levels of the first and second QD are -5.4 eV and -2.4 eV, respectively. The rectification is carried out, and it is illustrated in Fig. 3. We plotted the conductance as a function of the time, where it is measured in units $(2e^2/h)$ as shown in Fig. 3. From the yields, we evidently noted that conductance show limit value only in the positive half-cycles of the AC input voltage. From the other side, conductance precisely vanishes for the negative half-wave of the AC input voltage.

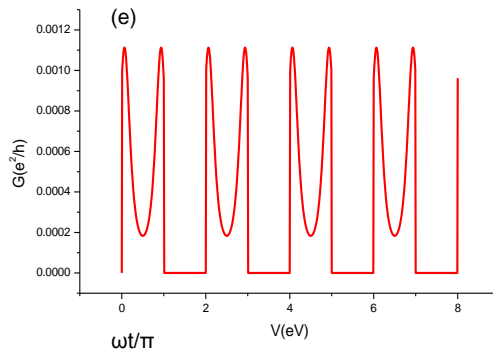
We also noted that every peak in the conductance spectrum has been split into two secondary peaks. This splitting appears obviously in Fig.3 that occurs due to the increase in the amplitude of input signal.

To describe the rectification process more clearly we display the variety of current as a function of the time as shown in Fig. 4. It measures with units $(2e/h)$. The current is getting through the diode by integrating over the transmission function, see Eq. 10. The non-vanishing behavior of current is only satisfied for the positive half-wave of the AC input signal for $n\pi < \omega t < (n + 1)\pi$, where n is zero or even. The vanishing nature of current in the negative half-wave input signal is evidently identify at $n\pi < \omega t < (n + 1)\pi$, where n is odd. Each of these characteristics evidently helps the half-wave rectification work when we obtain in conventional half-wave rectifiers. Characterizing an ADQD involves finding the I - V characteristic behavior of the ADQD for both the forward and the reverse bias modes of operation. A typical representation of the I - V characteristics for both modes of operation plotted on a linear scale is shown in Fig. 5. Initially, the current linearly changes with respect to the bias voltage. At a limit magnitude of bias voltage $V=7$ eV, the current is constant with the bias voltage. In other words, it becomes constant at forwarding bias condition. While at reverse bias condition the I - V characteristic curve vanishes on negative V axis. Further, it can be noticed that the peaks of the current do not change in shape with increasing of the amplitudes of input signal, but they increase in the value of current as shown in detail in Fig.4. There is a good agreement

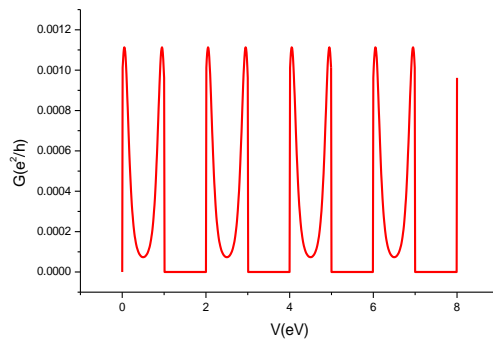
for our results with previous theoretical study [37]. Also, our results were obtained by using Mat-lab and FORTRAN self-designed codes.







(f)



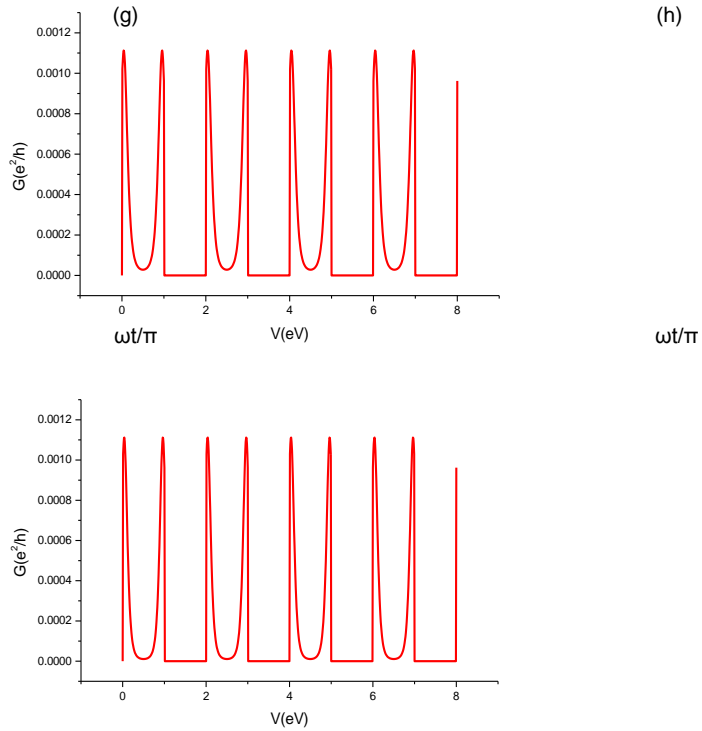


Fig. 3. The conductance as functions of the time after half-wave rectification action for different values of input signal as follow: $V=0.1, 0.25, 0.5, 0.75, 1.0, 1.25, 1.5$ and 1.75 eV for a, b, c, d, e, f, g and h panels respectively.

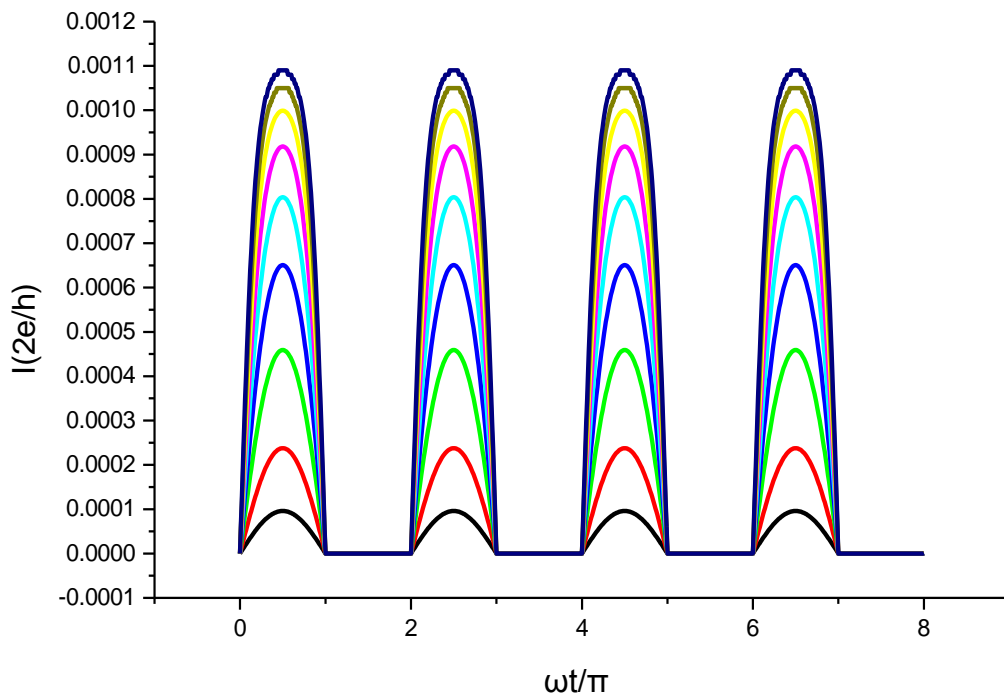


Fig. 4. The current as functions of the time after half-wave rectification action for different values of input signal as follow: $V=0.1, 0.25, 0.5, 0.75, 1.0, 1.25, 1.5, 1.75$ and 2.0 eV for black, red, green, blue, bright blue, pink, yellow, brown and dark blue respectively.

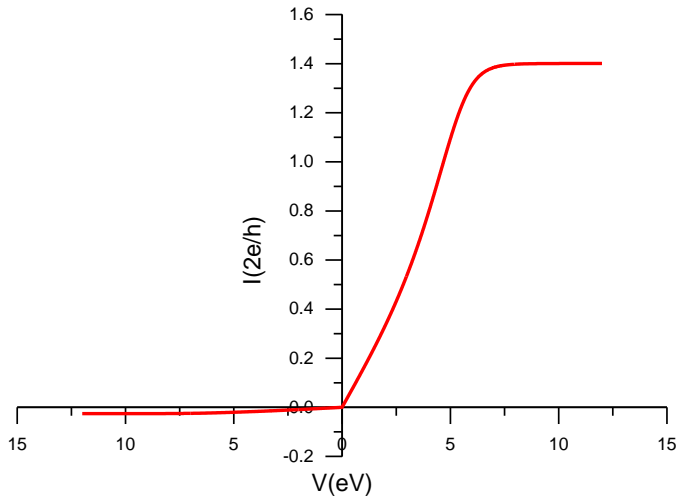


Fig. 5. Illustrate the *I-V* characteristics for ADQD.

4. CONCLUSION

We have presented the possibilities of designing nanoscale diode using ADQD structure. The half-wave rectifier is designed by using ADQD to examine the work of ADQD as a diode. The ADQD acts as diode very well, which seems clear in *I-V* characteristic. The rectification operation is achieved by using the central idea of arrangement QDs geometric. The ADQD are connected serially and that are asymmetrical in the sizes, one small and another big, so the ADQD structure has different gap energies. We used a tight-binding treatment to illustrate our model and every computation was carried out by using steady state formalism. The numerical consequences give conductance and current that avocation the basic characteristics of rectifications. Thus, the analysis can be used in designing nanoscale rectifiers.

ACKNOWLEDGEMENTS

We thank Prof. Jenan Majeed AL-Mukh and Prof. Shakier Ibraheem Easa from Basrah University for useful discussions. We also thank Iraqi Ministry of Higher Education and Scientific Research for its support of scientific researches through the Iraqi Virtual Science Library.

REFERENCES

- [1] Nozik AJ, Beard MC, Luther JM, Law M, Ellingson RJ, Johnson JC. Semiconductor quantum dots and quantum dot arrays and applications of multiple exciton generation to third-generation photovoltaic solar cells. *Chemical reviews*. 2010;110(11):6873-90.
- [2] Yang W-X, Chen A-X, Guo H, Bai Y, Lee R-K. Carrier-envelope phase control electron transport in an asymmetric double quantum dot irradiated by a few-cycle pulse. *Optics Communications*. 2014;328:96-101.
- [3] Wang Z, Yu B. Two-dimensional localization effect via spatial-dependent quantum interference in an asymmetric double quantum dot nanostructure. *JOSA B*. 2014;31(3):565-71.
- [4] Hiltunen T, Bluhm H, Mehl S, Harju A. Charge-noise tolerant exchange gates of singlet-triplet qubits in asymmetric double quantum dots. *Physical Review B*. 2015;91(7):075301.
- [5] Aviram A, Ratner MA. Molecular rectifiers. *Chemical Physics Letters*. 1974;29(2):277-83.
- [6] Launay JP. *Molecular electronics. Granular nanoelectronics*: Springer; 1991. p. 413-23.
- [7] Baer R, Neuhauser D. Phase coherent electronics: a molecular switch based on quantum interference. *Journal of the American Chemical Society*. 2002;124(16):4200-1.
- [8] Orellana PA, Dominguez-Adame F, Gomez I, de Guevara MLLn. Transport through a quantum wire with a side quantum-dot array. *Physical Review B*. 2003;67(8):085321.
- [9] Tagami K, Wang L, Tsukada M. Interface sensitivity in quantum transport through single molecules. *Nano letters*. 2004;4(2):209-12.

- [10] Cui WY, Wu SZ, Jin G, Zhao X, Ma YQ. Analytic study of electron transmission through serial mesoscopic metallic rings. *The European Physical Journal B*. 2007;59(1):47-54.
- [11] Pickup BT, Fowler PW. An analytical model for steady-state currents in conjugated systems. *Chemical Physics Letters*. 2008;459(1):198-202.
- [12] Maiti SK. Quantum transport in mesoscopic ring structures: Effects of impurities, long-range hopping and interactions. *Quantum Matter*. 2012;3(5):413-34.
- [13] Maiti SK. Externally controlled local magnetic field in a conducting mesoscopic ring coupled to a quantum wire. *Journal of Applied Physics*. 2015;117(2):024306.
- [14] Al-Badry LF. The influence of the nanostructure geometry on the thermoelectric properties. *Physica E: Low-dimensional Systems and Nanostructures*. 2016;83:201-6.
- [15] Fischer CM, Burghard M, Roth S, Klitzing Kv. Microstructured gold/Langmuir-Blodgett film/gold tunneling junctions. *Applied physics letters*. 1995;66(24):3331-3.
- [16] Reed MA, Zhou C, Muller CJ, Burgin TP, Tour JM. Conductance of a molecular junction. *Science*. 1997;278(5336):252-4.
- [17] Chen J, Reed MA, Rawlett AM, Tour JM. Large on-off ratios and negative differential resistance in a molecular electronic device. *Science*. 1999;286(5444):1550-2.
- [18] Dadosh T, Gordin Y, Krahne R, Khivrich I, Mahalu D, Frydman V, et al. Measurement of the conductance of single conjugated molecules. *Nature*. 2005;436(7051):677-80.
- [19] Imamura K, Sugiyama Y, Nakata Y, Muto S, Yokoyama N. New optical memory structure using self-assembled InAs quantum dots. *Japanese journal of applied physics*. 1995;34(11A):L1445.
- [20] Van Dyck C, Ratner MA. Molecular rectifiers: a new design based on asymmetric anchoring moieties. *Nano letters*. 2015;15(3):1577-84.

- [21] Xu H, Heinzl T, Zozoulenko IV. Electronic properties of quantum dots formed by magnetic double barriers in quantum wires. *Physical Review B*. 2011;84(3):035319.
- [22] Li M-J, Xu H, Chen K-Q, Long M-Q. Electronic transport properties in benzene-based heterostructure: Effects of anchoring groups. *Physics Letters A*. 2012;376(20):1692-7.
- [23] Trocha P, Barnaś J. Large enhancement of thermoelectric effects in a double quantum dot system due to interference and Coulomb correlation phenomena. *Physical Review B*. 2012;85(8):085408.
- [24] Gaudreau L, Granger G, Kam A, Aers GC, Studenikin SA, Zawadzki P, et al. Coherent control of three-spin states in a triple quantum dot. *Nature Physics*. 2012;8(1):54-8.
- [25] Rossella F, Bertoni A, Ercolani D, Rontani M, Sorba L, Beltram F, et al. Nanoscale spin rectifiers controlled by the Stark effect. *Nature nanotechnology*. 2014;9(12):997-1001.
- [26] Weber B, Tan YH, Mahapatra S, Watson TF, Ryu H, Rahman R, et al. Spin blockade and exchange in Coulomb-confined silicon double quantum dots. *Nature nanotechnology*. 2014.
- [27] Scott GD, Natelson D, Kirchner S, Muñoz E. Transport characterization of Kondo-correlated single-molecule devices. *Physical Review B*. 2013;87(24):241104.
- [28] Aligia AA, Roura-Bas P, Florens S. Impact of capacitance and tunneling asymmetries on Coulomb blockade edges and Kondo peaks in nonequilibrium transport through molecular quantum dots. *Physical Review B*. 2015;92(3):035404.
- [29] F Al-Badry L. AND gate response in a double mesoscopic ring. *Recent Patents on Nanotechnology*. 2017;11(1):63-9.
- [30] Datta S. *Quantum transport: atom to transistor*: Cambridge University Press; 2005.
- [31] Ellenbogen JC, Love JC. Architectures for molecular electronic computers. I. Logic structures and an adder designed from molecular electronic diodes. *Proceedings of the IEEE*. 2000;88(3):386426.
- [32] Maiti SK. Electron transport through mesoscopic rings: Evidence of nano-scale rectifiers. *Solid State Communications*. 2010;150(37):1741-5.

[33] G. Cuniberti, E. Maci, A. Rodriguez, and R.A. Romer , " Tight-binding modeling of charge

migration in DNA devices", Cornell I University Library, 2007.

[34] B. Giese, J. Amaudrut, A. Köhler, M. Spormann, and S. Wessely, Nature 412, 318 (2001).

[35] X.-Q. Li and Y. Yan, Appl. Phys. Lett., 79, 14, 2001.

[36] R. Gutierrez, S. Mandal, and G. Cuniberti, Physical Review B 71, I 235116 , 2005.

[37] M. H. Moaiyeri, K. Navi, O. Hashemipour, International Journal of Computer

Applications (0975 – 8887) Volume 64– No.2, February 2013.